

Electronic Supplementary Information for

Iron Polypyridyl Catalysts Assembled on Metal Oxide Semiconductors for Photocatalytic Hydrogen Generation

Nicholas A. Race, Wanji Zhang, Megan E. Screen, Brett A. Barden, and William R. McNamara*
Department of Chemistry, The College of William and Mary, Williamsburg VA

*Correspondence to: wrmcnamara@wm.edu

Table of Contents

Materials and Methods	4
Scheme S1 Synthesis of 4	4
Scheme S2 Synthesis of 5	5
Scheme S3 Synthesis of 2	6
Calculation of binding of 2 to TiO ₂ and SrTiO ₃	8
Figure S1 Calibration curve	10
Calculation of TON	10
Figure S2 ¹ H NMR of 2	11
Figure S3 ¹³ C NMR of 2	12
Figure S4 HR-MS of 2	13
Figure S5 Diffuse reflectance spectra of SrTiO ₃ , 2 -SrTiO ₃ , 3 -SrTiO ₃	14
Figure S6 Diffuse reflectance spectra of ZrO ₂ , 2 -ZrO ₂ , 3 -ZrO ₂	15
Figure S7 Diffuse reflectance spectra of TiO ₂ , fluorescein-TiO ₂	16
Figure S8 Diffuse reflectance spectra of SrTiO ₃ , fluorescein-SrTiO ₃	17
Figure S9 Diffuse reflectance spectra of TiO ₂ , Fe-TiO ₂	18
Figure S10 Diffuse reflectance spectra of SrTiO ₃ , Fe-SrTiO ₃	19
Figure S11 Powder ATR-FTIR spectra of 2 -TiO ₂ , 3 -TiO ₂	20
Figure S12 Powder ATR-FTIR spectra of 2 -SrTiO ₃ , 3 -SrTiO ₃	21
Figure S13 Powder ATR-FTIR spectra of TiO ₂ , fluorescein-TiO ₂	22
Figure S14 Powder ATR-FTIR spectra of SrTiO ₃ , fluorescein-SrTiO ₃	23
Figure S15 UV-Vis spectra of 2 -TiO ₂ binding study	24
Figure S16 UV-Vis spectra of 2 -SrTiO ₃ binding study	25
Figure S17 Hydrogen evolution of 3 -TiO ₂ and 3 -SrTiO ₃	26
Figure S18 UV-Vis spectra of 1 at varying pH	27
Table S1 Optimization of mass of 3 -TiO ₂ and 3 -SrTiO ₃ for hydrogen evolution	28
Figure S19 Optimization of fluorescein concentration with 3 -SrTiO ₃ for hydrogen evolution	29

Table S2 Additional control experiments	30
Table S3 Optimization of pH of sacrificial donor solution for hydrogen evolution	31
Figure S20 Emission spectra of fluorescein on TiO ₂ and SrTiO ₃	32
Figure S21 Catalyst stability study	33
References	34

Materials and Methods

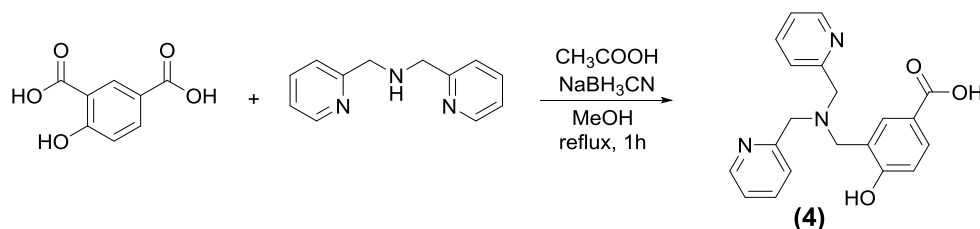
Materials

P25 TiO₂ was obtained from Acros Organics. Zirconia (diameter = 20 nm) was purchased from Sigma Aldrich. SrTiO₃ (diameter = 25 nm) was obtained from Alfa Aesar. Thin films of the metal oxides were prepared on microscope slides using a doctor blading technique.¹ Metal oxide films were used for diffuse reflectance UV-Vis spectroscopy. All other materials were used as received from Fisher Scientific.

Instrumentation

¹H and ¹³C NMR spectra were obtained using an Agilent 400MR DD2 spectrometer operating in the pulse Fourier transform mode. Chemical shifts are reported in ppm with the residual solvent as an internal reference. Mass spectrometry was carried out using positive electrospray ionization on a Bruker 12 Tesla APEX-Qe FTICR-MS with an Apollo II ion source. All GC analysis was performed using a Bruker Scion 436 gas chromatograph with argon carrier gas. All UV-Vis analysis was performed using an Agilent Cary 60 Spectrophotometer. IR analysis was performed using a Shimadzu IRTracer-100 FTIR with a MIRacle 10 Single Reflection ATR Accessory.

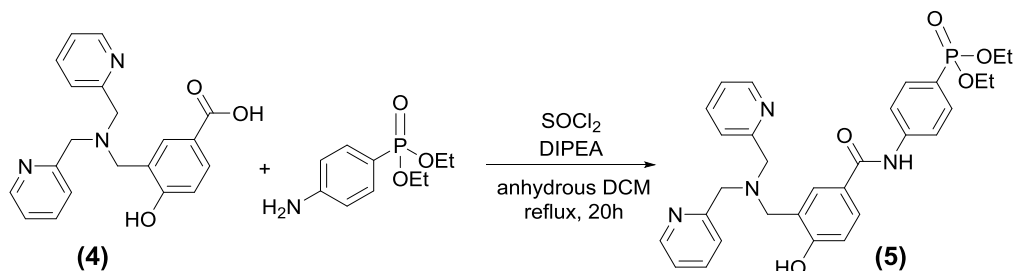
Syntheses



Scheme S1. Synthesis of 4.

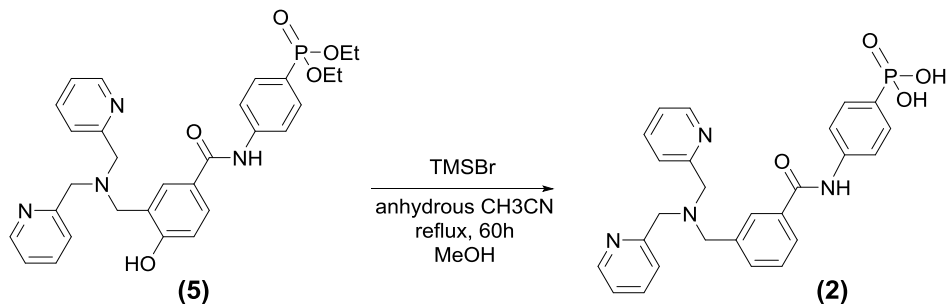
3-((bis(pyridin-2-ylmethyl)amino)methyl)-4-hydroxybenzoic acid (4). This compound was synthesized using a modified literature procedure.^{2,3} To a degassed solution of the benzoic acid (1.34 g, 8.1 mmol) in 10 mL of MeOH, a solution of bis(pyridine-2-ylmethyl)amine (1.46 mL, 8.1 mmol) in 4 mL of MeOH was added. To the resulting solution, 3 drops of glacial acetic acid was added followed by the addition of a solution of sodium cyanoborohydride (0.50 g, 8.1 mmol) in 4 mL of MeOH under argon. The resulting solution was allowed to reflux overnight. The solution was allowed to reach room temperature and 1 M HCl was added to the solution until it reached pH 4. The solution was evaporated to near dryness, dissolved in 50 mL of saturated NaHCO₃ solution and then extracted with dichloromethane (3 × 50 mL). 1 M HCl was added to the aqueous layer until it reached pH 7. The aqueous layer was extracted again with DCM (3 × 50 mL). The organic layers were combined, dried with MgSO₄, and filtered. The volatiles were

removed to give 0.81 g of **4** (29% yield). ^1H NMR (CDCl_3): 8.59 (m, 2H), 7.95 (dd, 1H), 7.86 (d, 1H), 7.67 (t, 2H), 7.35 (d, 2H), 7.21 (t, 2H), 6.95 (d, 1H), 3.95 (s, 4H), 3.85 (s, 2H). ^{13}C NMR (CDCl_3): 170.48, 162.47, 157.95, 148.31, 137.41, 131.89, 123.29, 122.50, 120.74, 116.71, 58.27, 56.76. HRMS for $\text{C}_{20}\text{H}_{19}\text{N}_3\text{O}_3\text{Na}^+$: predicted $m/z = 372.131863$, observed = 373.131849.



Scheme S2. Synthesis of **5**.

diethyl (4-(3-((bis(pyridin-2-ylmethyl)amino)methyl)-4-hydroxybenzamido)phenyl)phosphonate (5). This compound was synthesized using an adapted literature procedure.¹ To a solution of **4** (0.48 g, 1 mmol) in 40 mL of anhydrous DCM, SOCl_2 (0.22 mL, 3 mmol) was added dropwise. The resulting acid chloride solution was allowed to reflux for 2 h. The volatiles were then removed by liberally bubbling Ar through the solution. Diethyl (4-aminophenyl)phosphonate was prepared according to literature procedure.⁴ A solution containing DIPEA (0.42 mL, 1.04 mmol) and diethyl (4-aminophenyl)phosphonate (0.23 g, 1 mmol), in 40 mL of anhydrous DCM was added to the acid chloride solution. The resulting solution was allowed to reflux overnight. The brown solution was diluted with water (40 mL), extracted with ethyl acetate (3×40 mL), and washed with saturated NaHCO_3 solution (3×40 mL). The organic layer was dried with MgSO_4 and filtered. Upon removal of the volatiles, the brown solid residue was purified by column chromatography on silica gel. Elution with a 5% TEA in DCM and 10% MeOH in DCM, sequentially, afforded the separation of a brown band containing the ligand **5**. The product was dissolved in DCM and washed with water (3×40 mL) to remove TEA residue from the column. This afforded 0.15 g of **5** (63% yield). ^1H NMR (CDCl_3): 8.57 (dq, 2H), 7.78 (m, 4H), 7.71 (m, 2H), 7.65 (td, 2H), 7.32 (d, 2H), 7.19 (m, 2H), 6.97 (d, 1H), 4.10 (m, 4H), 3.93 (s, 4H), 3.86 (s, 2H), 1.31 (t, 6H). ^{13}C NMR (CDCl_3): 166.62, 161.66, 157.94, 148.30 (d, $J = 8$ Hz), 142.30 (d, $J = 16$ Hz), 136.99 (d, $J = 12$ Hz), 132.45 (d, $J = 180$ Hz), 130.34 (d, $J = 20$ Hz), 128.35 (d, $J = 16$ Hz), 124.57, 122.74 (d, $J = 768$ Hz), 123.40, 123.13, 122.35, 119.45 (d, $J = 60$ Hz), 116.91, 62.05 (d, $J = 20$ Hz), 58.82, 56.42, 16.30 (d, $J = 28$ Hz). HRMS for $\text{C}_{30}\text{H}_{33}\text{N}_4\text{O}_5\text{PH}^+$: predicted $m/z = 561.226133$, observed = 561.226049.



Scheme S3. Synthesis of **2**.

(4-(3-((bis(pyridin-2-ylmethyl)amino)methyl)-4-hydroxybenzamido)phenyl)phosphonic acid (2). To a solution of **5** (0.05 g, 0.089 mmol) in 4.5 mL of anhydrous CH₃CN, TMSBr (47 μ L, 0.36 mmol) was added dropwise. The resulting solution was allowed to reflux for 60 h. The reaction was quenched with 2 mL of MeOH. The volatiles were removed to yield a brown solid. The solid was recrystallized in isopropanol to give 18 mg of **2** (42% yield). ¹H NMR (CD₃OD): 8.77 (d, 2H), 8.34 (dt, 2H), 7.96 (d, 2H), 7.90 (m, 3H), 7.80 (m, 4H), 7.69 (dd, 1H), 6.74 (d, 1H), 4.52 (s, 4H), 4.06 (s, 2H). ¹³C NMR (CD₃OD): 166.40, 159.35, 152.87, 144.15, 143.08, 141.86 (d, J = 12 Hz), 132.23, 131.30 (d, J = 36 Hz), 129.94, 128.44 (d, J = 472 Hz), 126.00, 125.58, 125.28, 120.78, 119.90 (d, J = 60 Hz), 114.81, 57.16, 54.32. HRMS for C₂₆H₂₅N₄O₅PNa⁺: predicted m/z = 505.163533, observed = 505.163539

Photochemistry Studies

Sensitization Procedure. Catalyst was immobilized on the semiconductor surface by soaking nanoparticles in a methanolic solution of ligand, followed by centrifugation. The ligand-sensitized nanoparticles were then exposed to a solution of FeCl₃ in methanol to form the active catalysts. A typical preparation is outlined below:

A measured amount (20-60 mg) of semiconductor nanoparticles along with excess ligand solution (1.0 x 10⁻⁷ moles ligand in methanol per 5 mg of semiconductor) was added to a sample vial. Excess methanol was added to the sample vial to bring the total volume to 5.0 mL. The sample vial was stirred for one hour. After stirring, the mixture was divided into microcentrifuge tubes and centrifuged at 13,400 rpm for 15 minutes. The supernatant was removed, followed by the addition of methanol to the centrifuge tubes to rinse the nanoparticles. The mixtures were then stirred and sonicated prior to being centrifuged for three minutes. The previously described wash process involving the three minute centrifugation was completed a total of four times. Following the final centrifugation of samples, the supernatant was removed and the ligand-sensitized nanoparticles were transferred to a clean sample vial with a stir bar. Excess FeCl₃ solution (1.0 x 10⁻⁷ moles in methanol per 5 mg of semiconductor) was added to the sample vial along with excess methanol to bring the total volume to 5.0 mL. The sample vial was sealed and stirred for one hour. During this process a color change of the mixture was observed from white to pale purple. After stirring, the mixture was subjected to the identical centrifuge and wash procedure as previously outlined with the ligand immobilization. Following the final

centrifugation of samples, the supernatant was removed and the nanoparticles were allowed to dry overnight in the dark.

Hydrogen Evolution Studies. Samples for hydrogen evolution were prepared in test tubes with final ratios of 1:1 ethanol:water as the solvent. These solutions contained 1 mg of catalyst-functionalized nanoparticles, 2 mM fluorescein, and 5% triethylamine by volume. Following addition of triethylamine solution, test tubes were capped with septa and sealed with copper wire. Samples were then degassed for 10 minutes with argon in the dark. A Hamilton gas syringe was then used to remove 1.0 mL of headspace from each test tube and add 1.0 mL methane as an internal standard. Test tubes were then irradiated with green light-emitting diodes ($\lambda = 520$ nm, 0.12 W) while stirring mixtures for a predetermined amount of time. After irradiation, a Hamilton gas syringe was used to remove 0.10 mL of headspace gas from each test tube and injected into a gas chromatograph for analysis.

Stability Studies. Samples were prepared in identical fashion to hydrogen evolution studies with 5 mg of catalyst-functionalized nanoparticles were added to each sample rather than 1 mg. Degassing, irradiation, and headspace gas analysis were performed in identical fashion to hydrogen evolution studies. Following 31 hours of irradiation, samples were removed from the green LED setup and centrifuged at 5,000 rpm for 12 minutes. Following centrifugation, the solution was removed from each sample, rinsed with EtOH, and fresh fluorescein solution was added. Samples were then capped with septa and sealed with copper wire. A syringe was then used to add triethylamine solution to samples, followed immediately by degassing for 10 minutes with argon in the dark. After degassing, a Hamilton gas syringe was used to remove 1.0 mL of headspace from each test tube and add 1.0 mL methane as an internal standard. Test tubes were then placed back in green LED setup for irradiation while stirring. A Hamilton gas syringe was used to remove 0.10 mL of headspace gas from each test tube and injected into a gas chromatograph for analysis at specific time intervals.

Control Experiments

Photolysis of 2-TiO₂ and 2-SrTiO₃ (no iron). Ligand was immobilized on the semiconductor surface through a centrifuge process as previously outlined. After final centrifugation of the mixture, supernatant was removed and microcentrifuge tubes containing ligand-immobilized nanoparticles were left to dry in the dark overnight. These nanoparticles were then used for photochemistry experiments under optimal conditions for hydrogen generation.

Photolysis of Bare metal oxide treated with FeCl₃ (no ligand). TiO₂ and SrTiO₃ thin films were placed in a petri dish wrapped in aluminum foil. Excess (8.0×10^{-7} moles) FeCl₃ in methanol was added to petri dish along with excess methanol to submerge thin film. The petri dish was then covered with a watch glass and aluminum foil cover to prevent light exposure. Thin film was soaked for 30 minutes. After soaking, the thin film was removed from the petri dish and rinsed with methanol. The films were then allowed to dry overnight. These nanoparticles were then used for photochemistry experiments under optimal conditions for hydrogen generation.

Photolysis of 3-TiO₂ and 3-SrTiO₃ without chromophore (no chromophore). Catalyst was immobilized on semiconductor surface through centrifuge process as previously outlined. 2.0 mL ethanol added to each test tube rather than fluorescein solution to maintain 1:1 ethanol:water mixture. All other conditions and procedures performed in identical manner to previously described photochemistry experiments.

No semiconductor. Identical concentration of **2** and FeCl₃ as measured to be on 1 mg NPs added directly to test tubes containing no semiconductor. Photochemistry experiment then performed under optimal conditions for hydrogen generation.

Surface Coverage Determination

UV-Vis was used to determine the coverage of ligand on the metal oxide semiconductors as outlined in previously reported procedures.⁵ A 2.5×10^{-5} M ligand solution in methanol was prepared and analyzed via UV-Vis spectrophotometry. 4.0 mL of the ligand solution was then added to a sample vial with 5.0 mg of semiconductor. The sample vial was capped and then stirred for one hour. The mixture was then divided into microcentrifuge tubes and centrifuged at 13,400 rpm for 15 minutes. After centrifugation, the supernatant was collected and analyzed via UV-Vis spectrophotometry. The absorbance of the supernatant was compared to the absorbance of the original ligand solution at 295 nm. The difference in absorbance at 295 nm between the ligand stock solution and supernatant was used to calculate the number of moles of ligand immobilized on the semiconductor surface. A sample calculation is shown below:

$$\text{mol } \mathbf{2} = \left[1 - \left(\frac{\text{supernatant absorbance}}{\text{original ligand solution absorbance}} \right) \right] \times (2.5 \times 10^{-5} M) \times (4 \times 10^{-3} L)$$

$$\text{mol } \mathbf{2} = \left[1 - \left(\frac{0.047917}{0.324828} \right) \right] \times (2.5 \times 10^{-5} M) \times (4 \times 10^{-3} L)$$

$$\text{mol } \mathbf{2} = 8.52 \times 10^{-8} \text{ moles per 5 mg nanoparticles}$$

Preparation of Thin Films

Film preparation (doctor blading). Semiconductor and deionized water were added to a sample vial in 4.0 g : 7.0 mL ratio. The mixture stirred for at least four hours to form a slurry. After stirring, the mixture was transferred onto microscope slides using a Pasteur pipette on one side of the microscope slide. The metal oxide slurry was then whisked across the microscope slide with a razor blade to give a thin even layer. The resulting thin films were then cured in a muffle furnace at 300 °F for two hours.

Sensitization of thin films. After cooling, the thin film was placed in an aluminum foil wrapped petri dish. 8×10^{-7} moles of ligand were added to the petri dish along with excess methanol to ensure thin film is completely submerged. The petri dish was then covered with a watch glass and aluminum foil to prevent light exposure. The thin film soaked in ligand solution for 30 minutes. After soaking, the thin film was removed from the petri dish and rinsed with methanol and dichloromethane. The petri dish was also rinsed with methanol prior to returning the thin film to petri dish. 8×10^{-7} moles of FeCl₃ was then added to the petri dish, along with

excess methanol to ensure thin film is fully submerged. The dish was covered with a watch glass and aluminum foil to prevent light exposure. The thin film was allowed to soak in FeCl_3 solution for 30 minutes. After soaking, the thin film was removed from the petri dish and rinsed with methanol and dichloromethane and then placed in a dark laboratory drawer to dry before use.

Calculation of Turnover Number

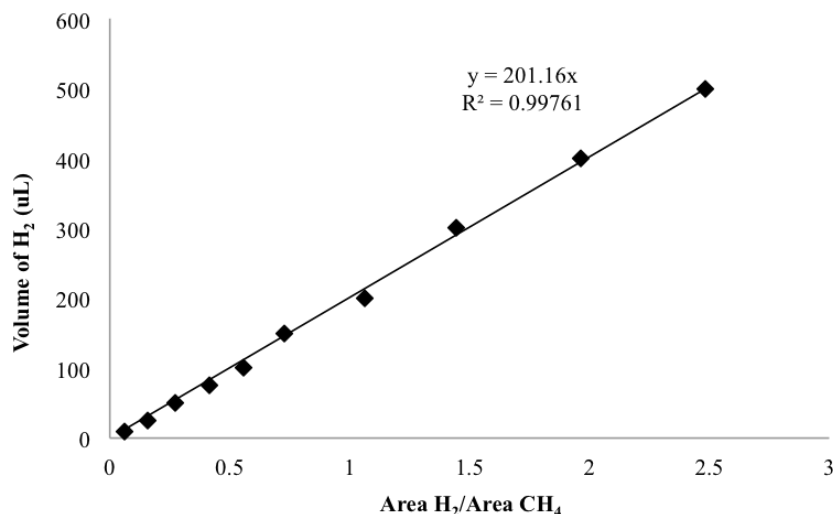


Figure S1. Calibration curve of H₂ to CH₄ peak areas used for determination of hydrogen generation. The ratio of peak areas was plotted against the volume of H₂ injected into the GC.

For our purposes, turnover number (TON) may be defined as the number of moles of hydrogen generated per mole of catalyst present in the system. We have previously developed a calibration curve relating the ratio of the peak areas of H₂ and CH₄ from our GC analysis to the volume of hydrogen generated by the system within our reaction vessel. Our calibration curve shows that the volume of hydrogen generated by the system has a linear relationship to the peak area ratio of the H₂ to CH₄ with a slope of 201.16, as shown by the relationship⁶:

$$\mu\text{L H}_2 = 201.16 \left(\frac{\text{Area H}_2}{\text{Area CH}_4} \right)$$

A sample calculation is included below:

$$\begin{aligned} \mu\text{L H}_2 &= 201.16 \left(\frac{525021}{35747.5} \right) = 2954 \\ 2954 \mu\text{L H}_2 &\times \frac{1 \text{ L}}{1 \times 10^6 \mu\text{L}} \times \frac{1 \text{ mol}}{22.4 \text{ L}} = 1.32 \times 10^{-4} \text{ mol H}_2 \\ \frac{1.32 \times 10^{-4} \text{ mol H}_2}{1.68 \times 10^{-8} \text{ mol catalyst}} &= 7850 \text{ TON} \end{aligned}$$

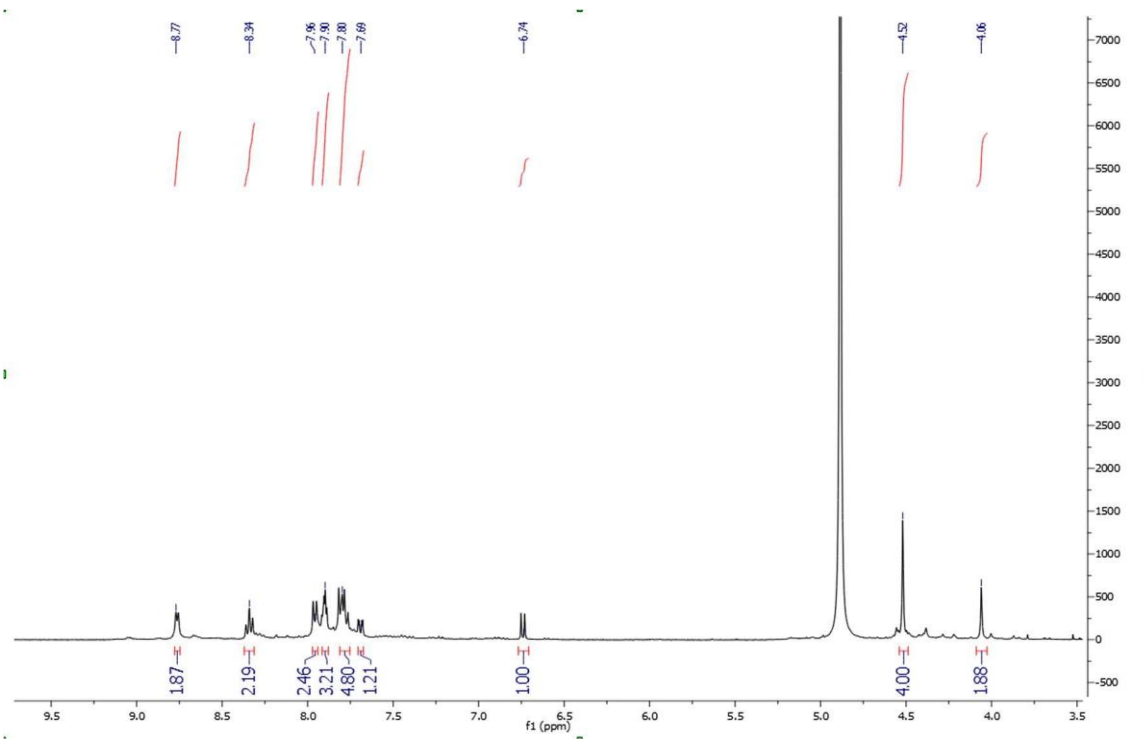


Figure S2. ¹H NMR spectrum of **2** with integrations in blue.

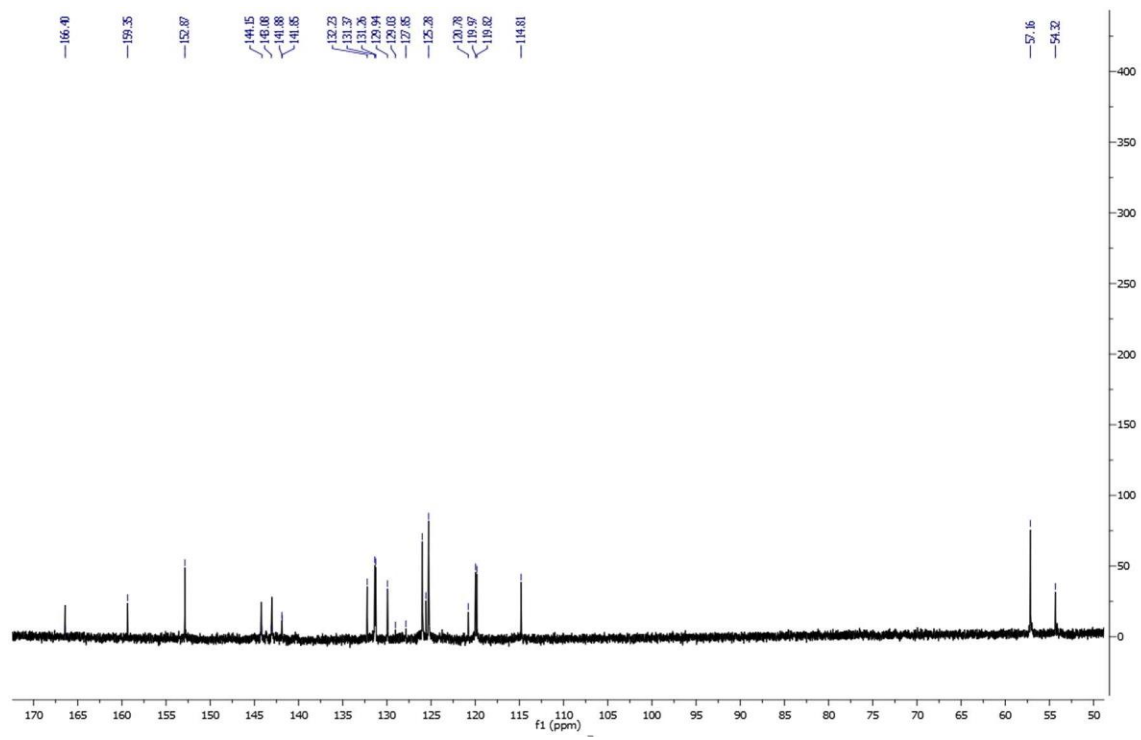


Figure S3. ^{13}C NMR spectrum of **2**.

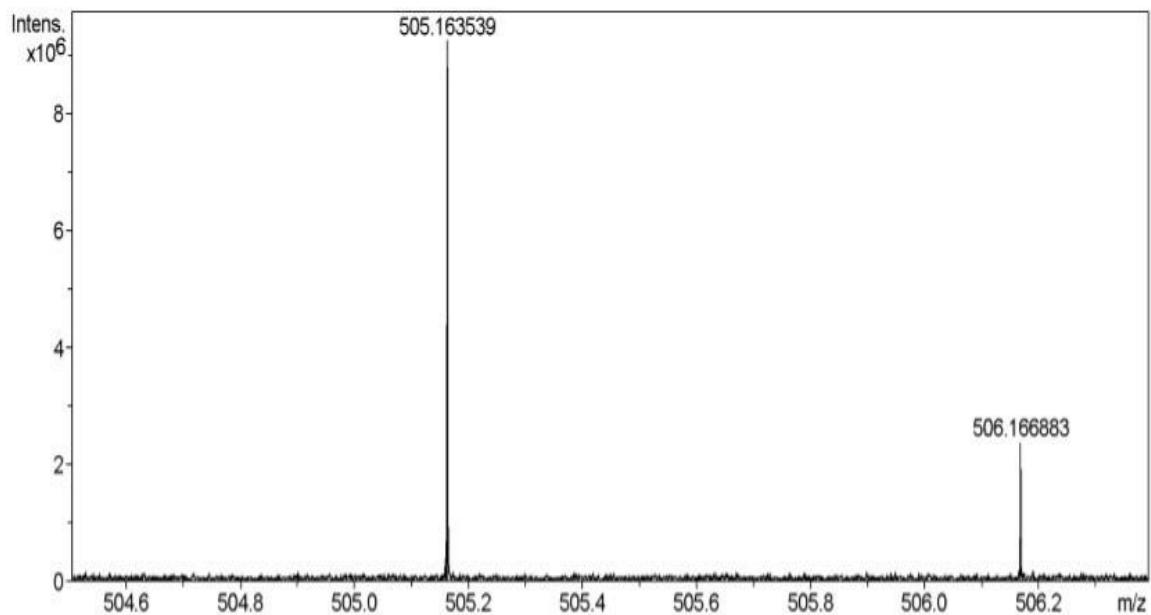


Figure S4. High-resolution mass spectrum of **2** in 1:1 THF:MeOH w/ NaCl. The expected molecular ions were observed with a difference of less than 1 ppm. Exact mass of $\text{C}_{26}\text{H}_{25}\text{N}_4\text{O}_5\text{PNa}^+$ = 505.163533 m/z Exact mass observed = 505.163539 m/z

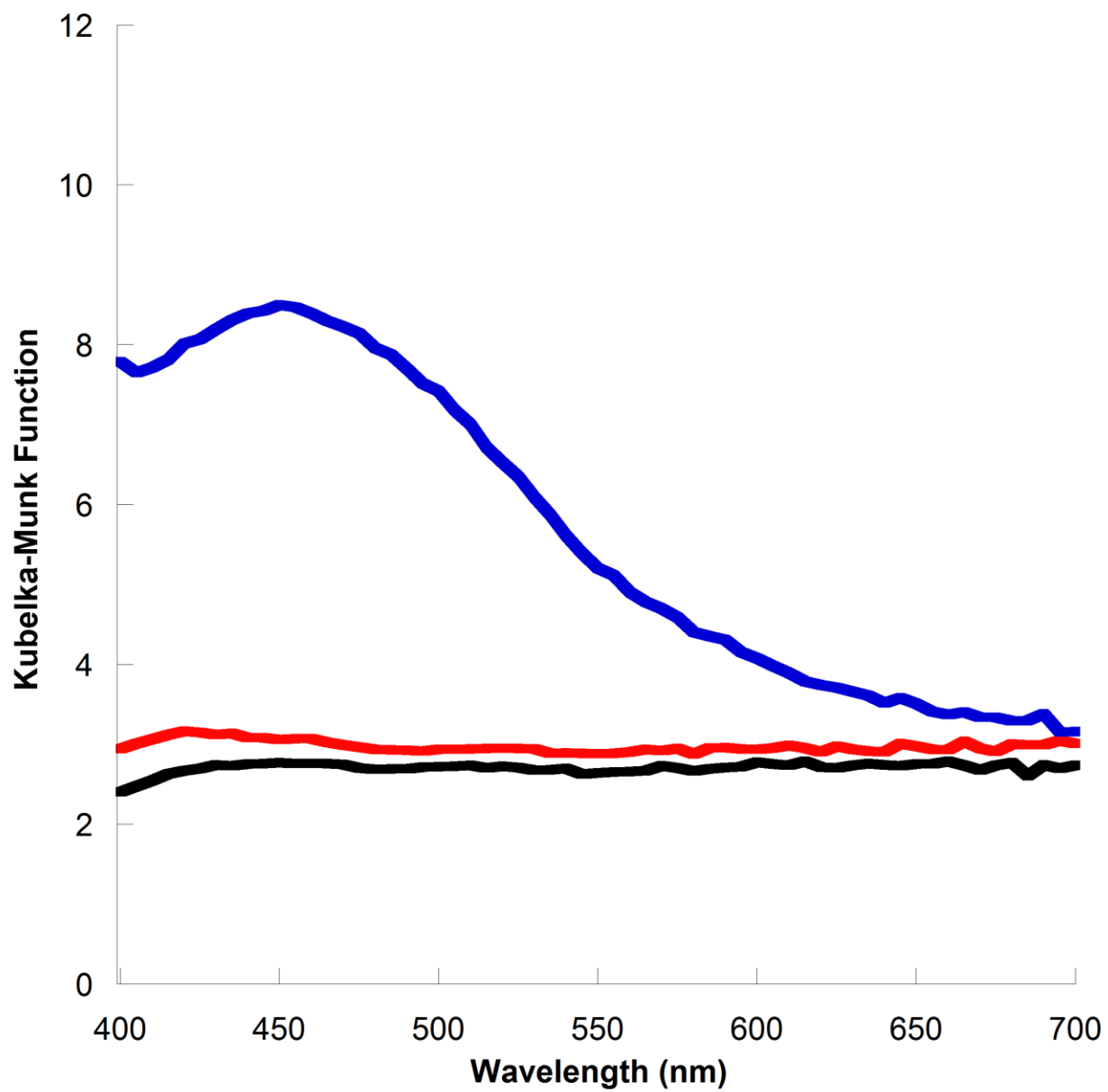


Figure S5. Diffuse Reflectance UV-Vis spectra of thin film of bare SrTiO₃ (black), 2-SrTiO₃ (red), and 3-SrTiO₃ (blue).

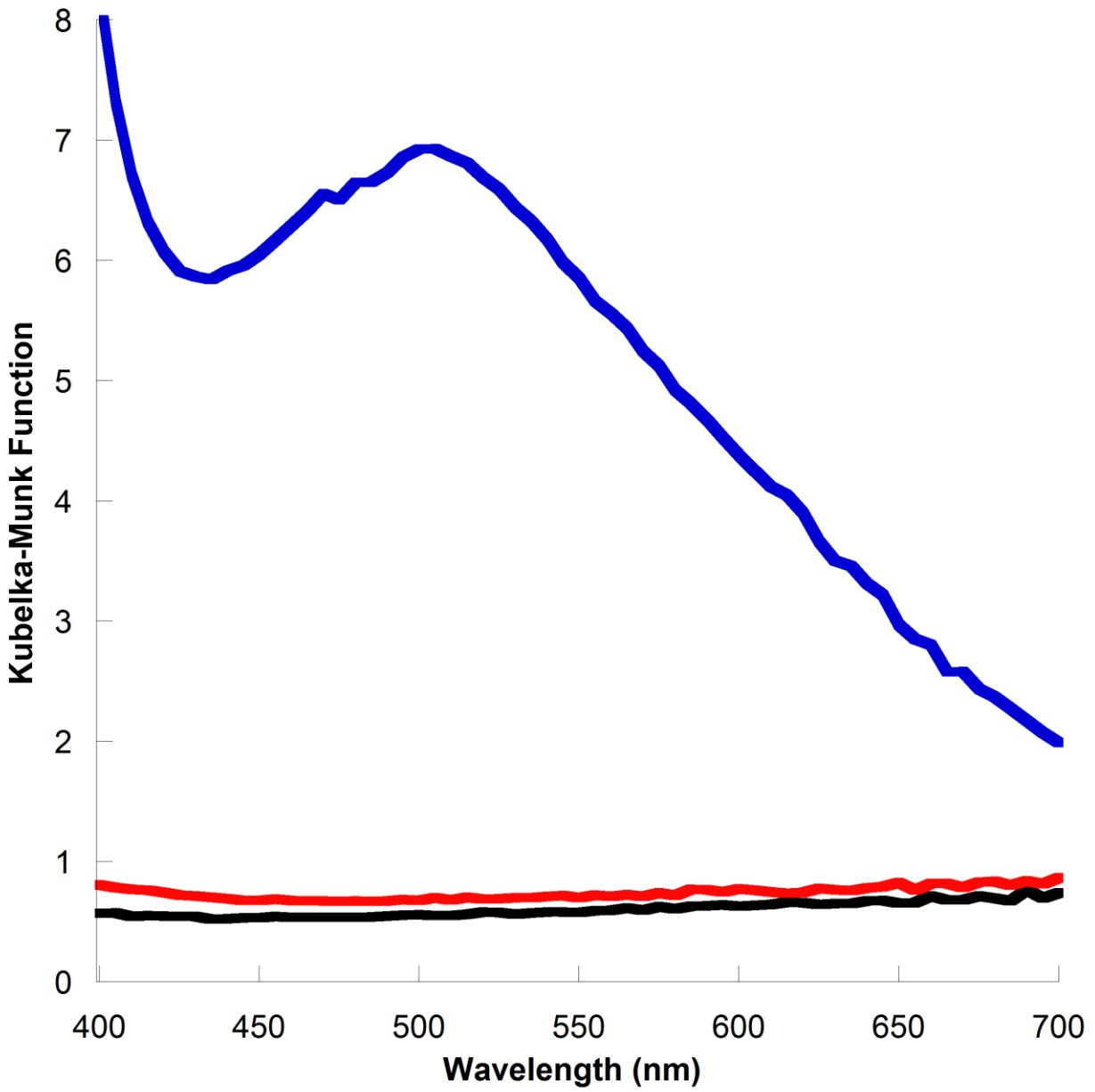


Figure S6. Diffuse Reflectance UV-Vis spectra of thin film of bare ZrO₂ (black), 2-ZrO₂ (red), and 3-ZrO₂ (blue).

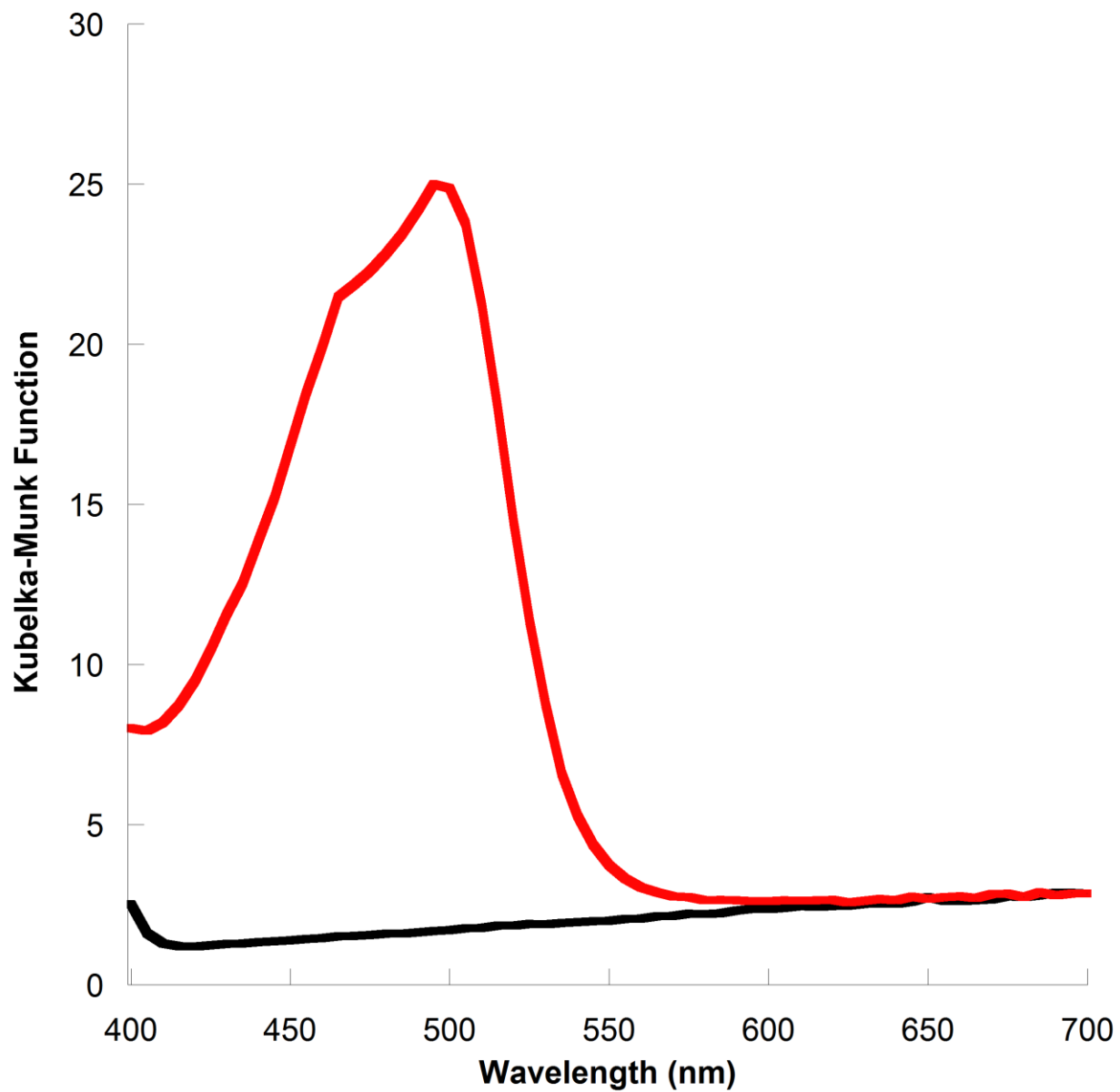


Figure S7. Diffuse Reflectance UV-Vis spectra of thin film of bare TiO₂ (black) and TiO₂ thin film sensitized with fluorescein (red).

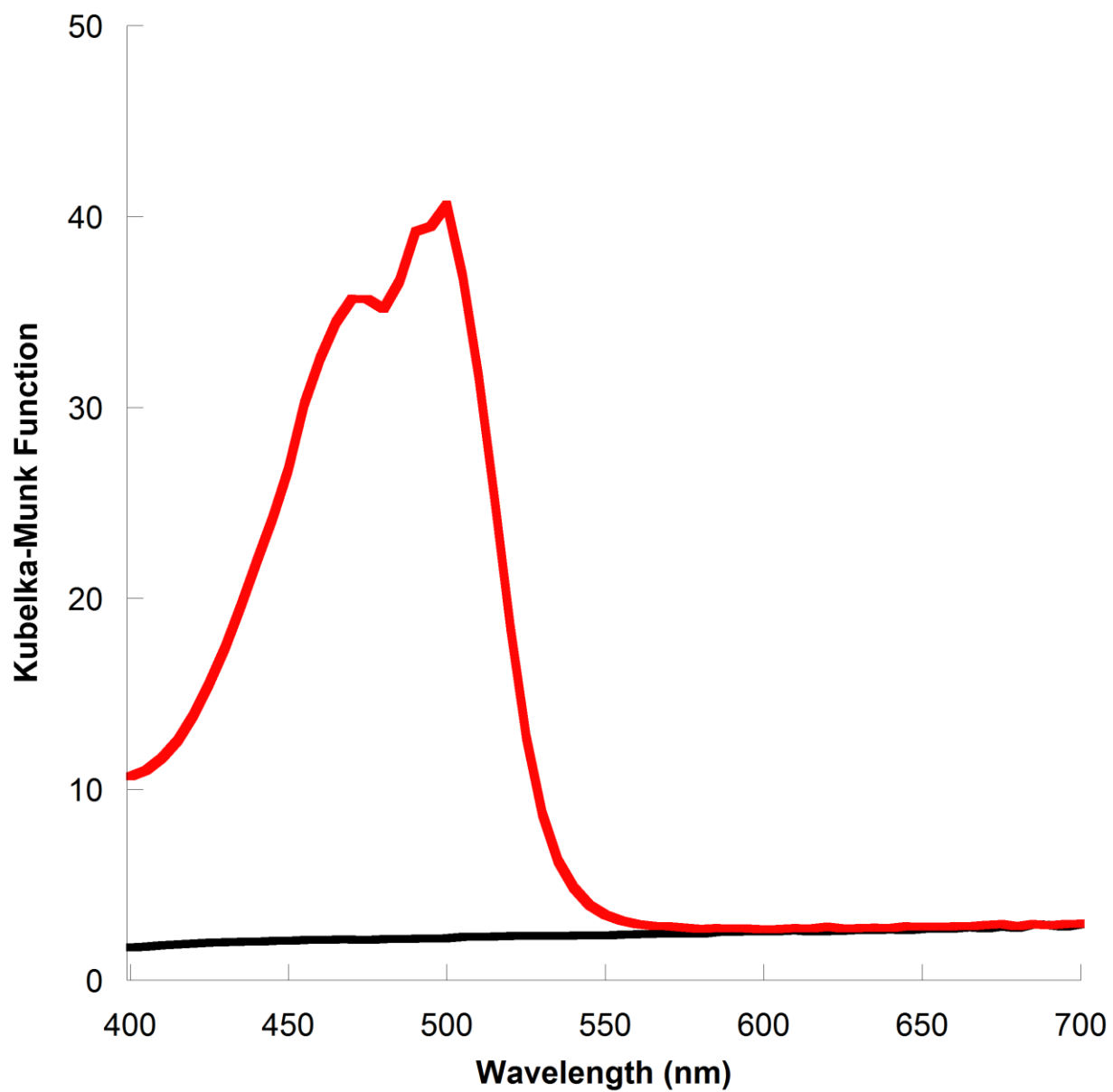


Figure S8. Diffuse Reflectance UV-Vis spectra of thin film of bare SrTiO₃ (black) and SrTiO₃ thin film sensitized with fluorescein (red).

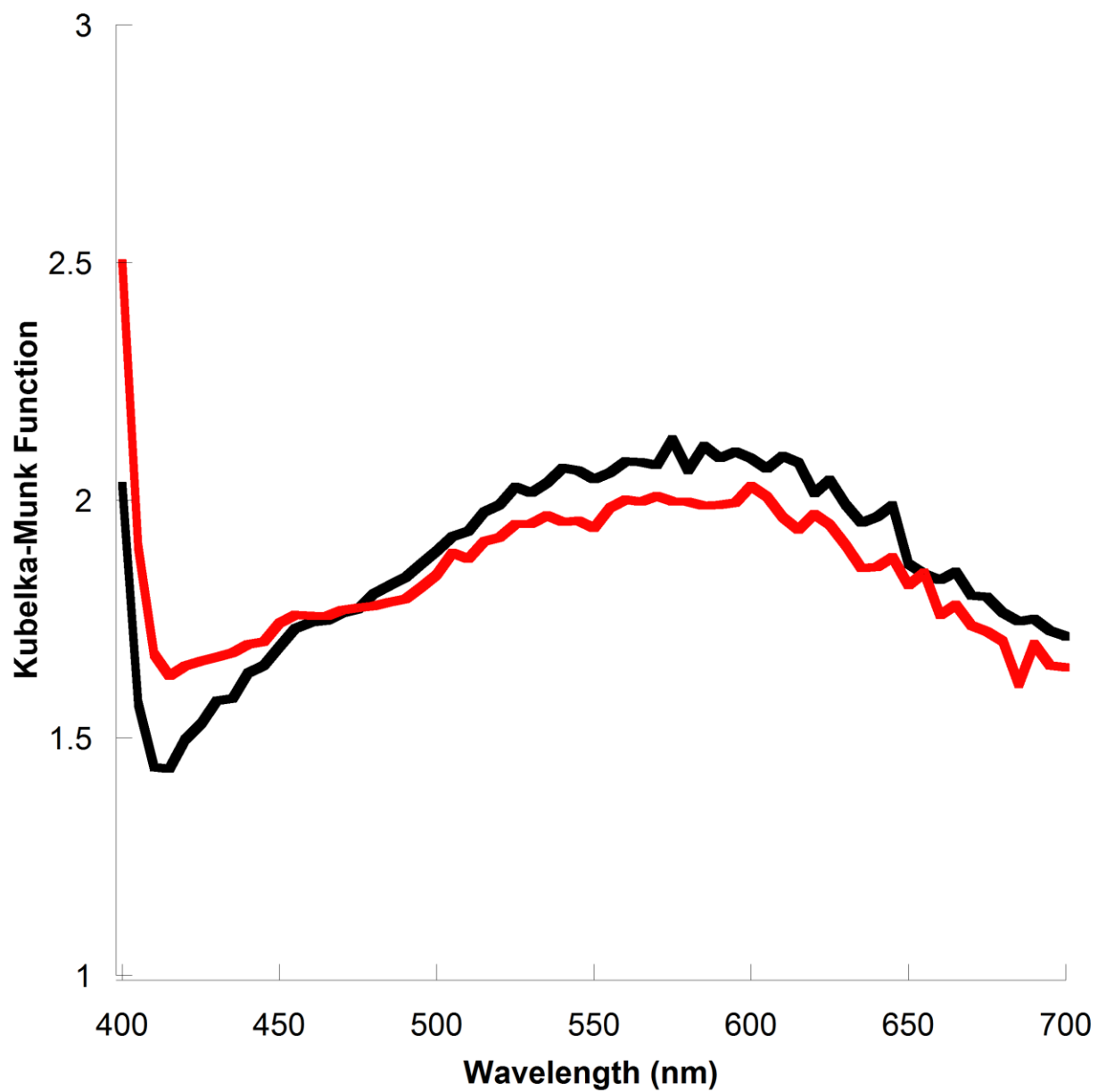


Figure S9. Diffuse Reflectance UV-Vis spectra of thin film of bare TiO₂ (black) and TiO₂ thin film sensitized with FeCl₃ (red).

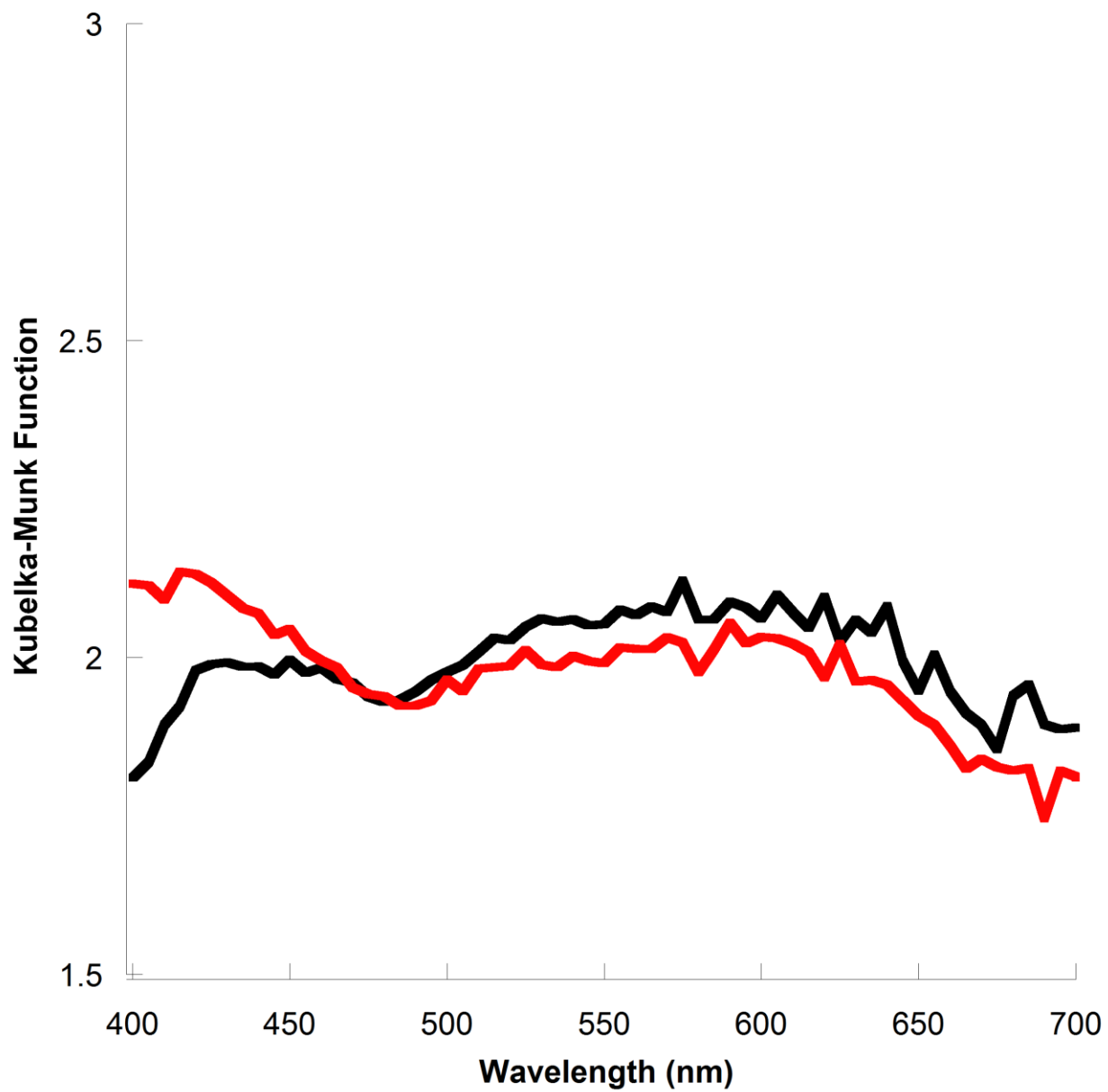


Figure S10. Diffuse Reflectance UV-Vis spectra of thin film of bare SrTiO₃ (black) and SrTiO₃ thin film sensitized with FeCl₃ (red).

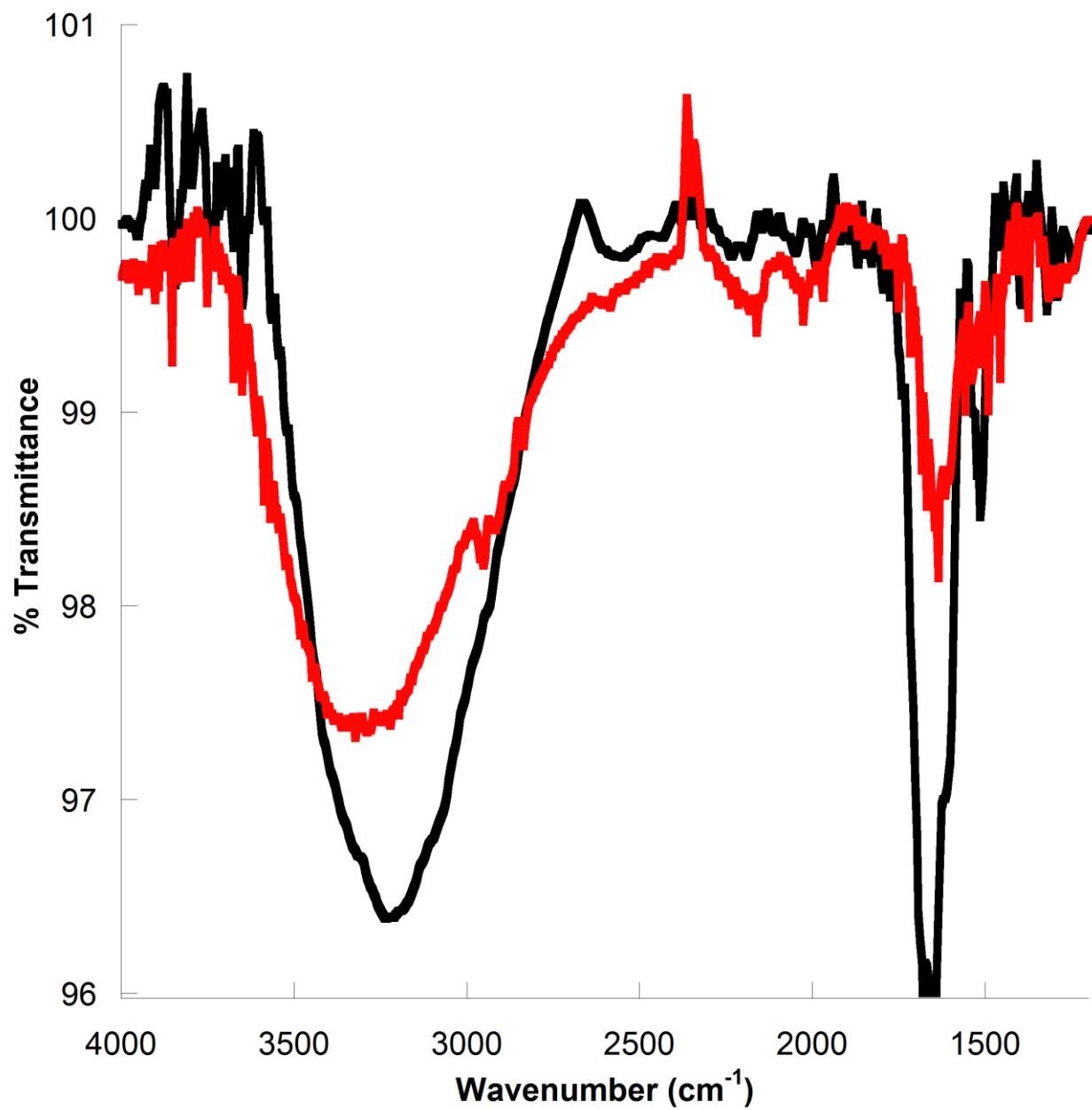


Figure S11. Powder ATR-FTIR spectra of 2-TiO₂ (black) and 3-TiO₂ (red).

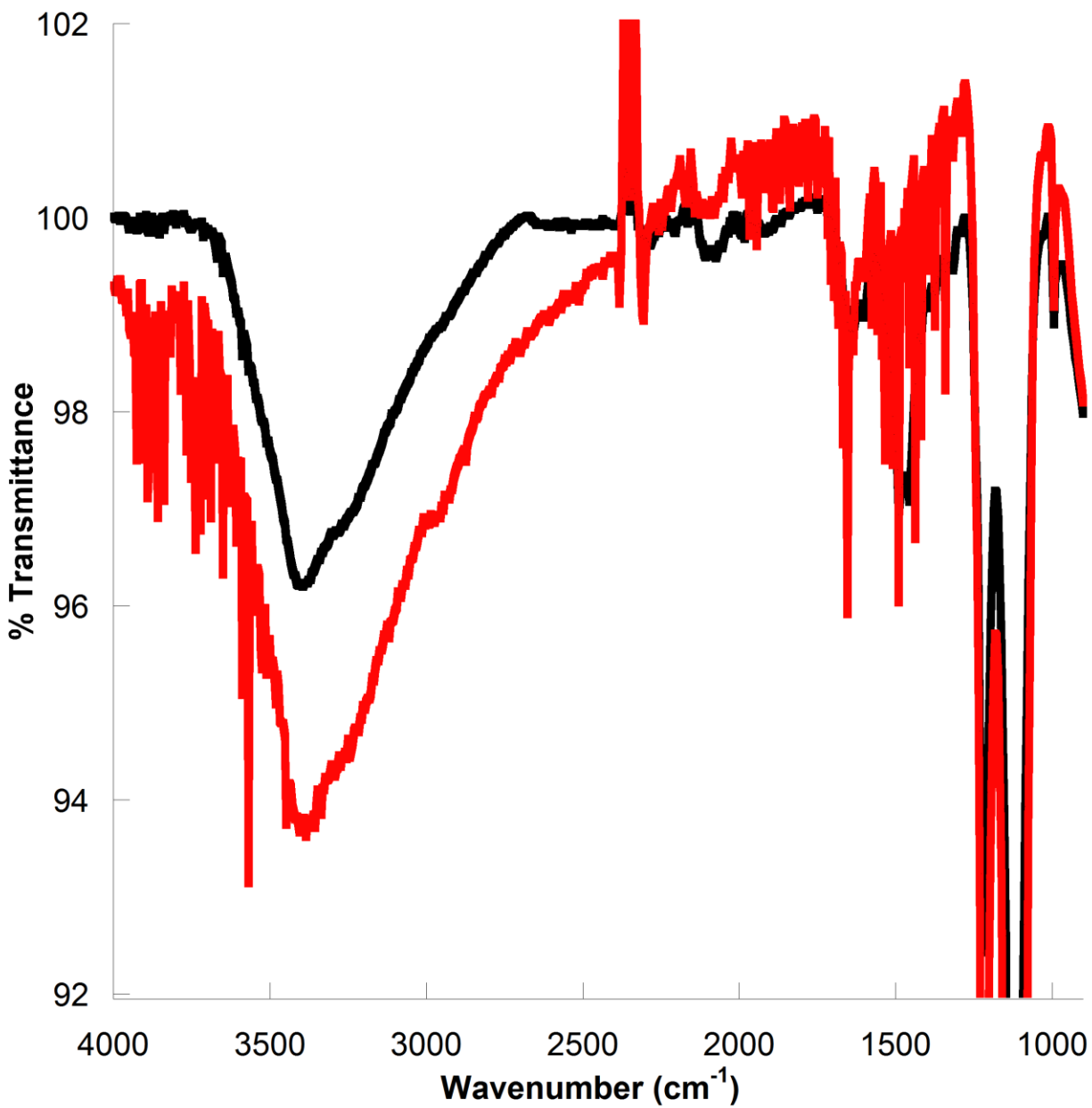


Figure S12. Powder ATR-FTIR spectra of 2-SrTiO₃ (black) and 3-SrTiO₃ (red).

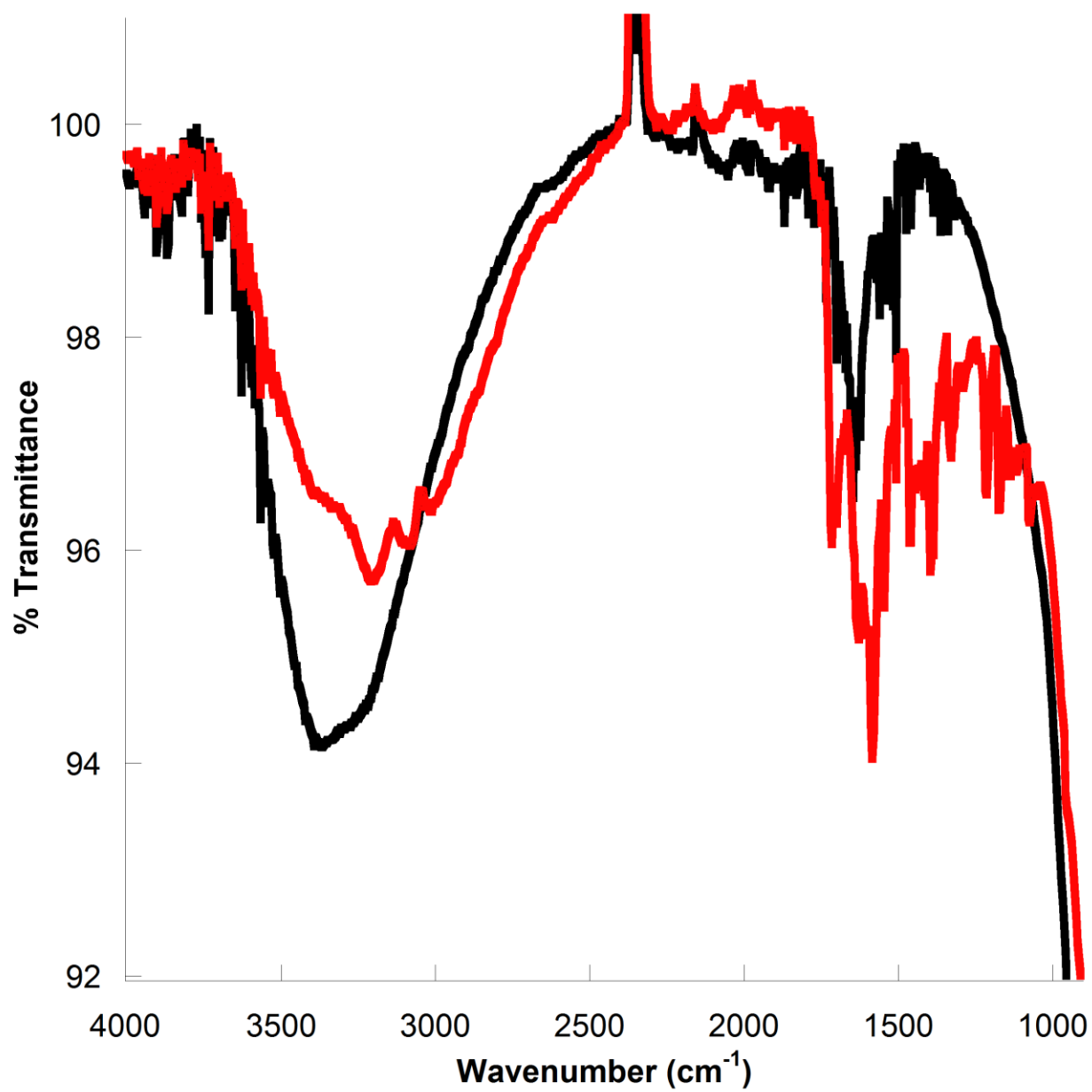


Figure S13. Powder ATR-FTIR spectra of TiO₂ (black) and TiO₂ sensitized with fluorescein (red).

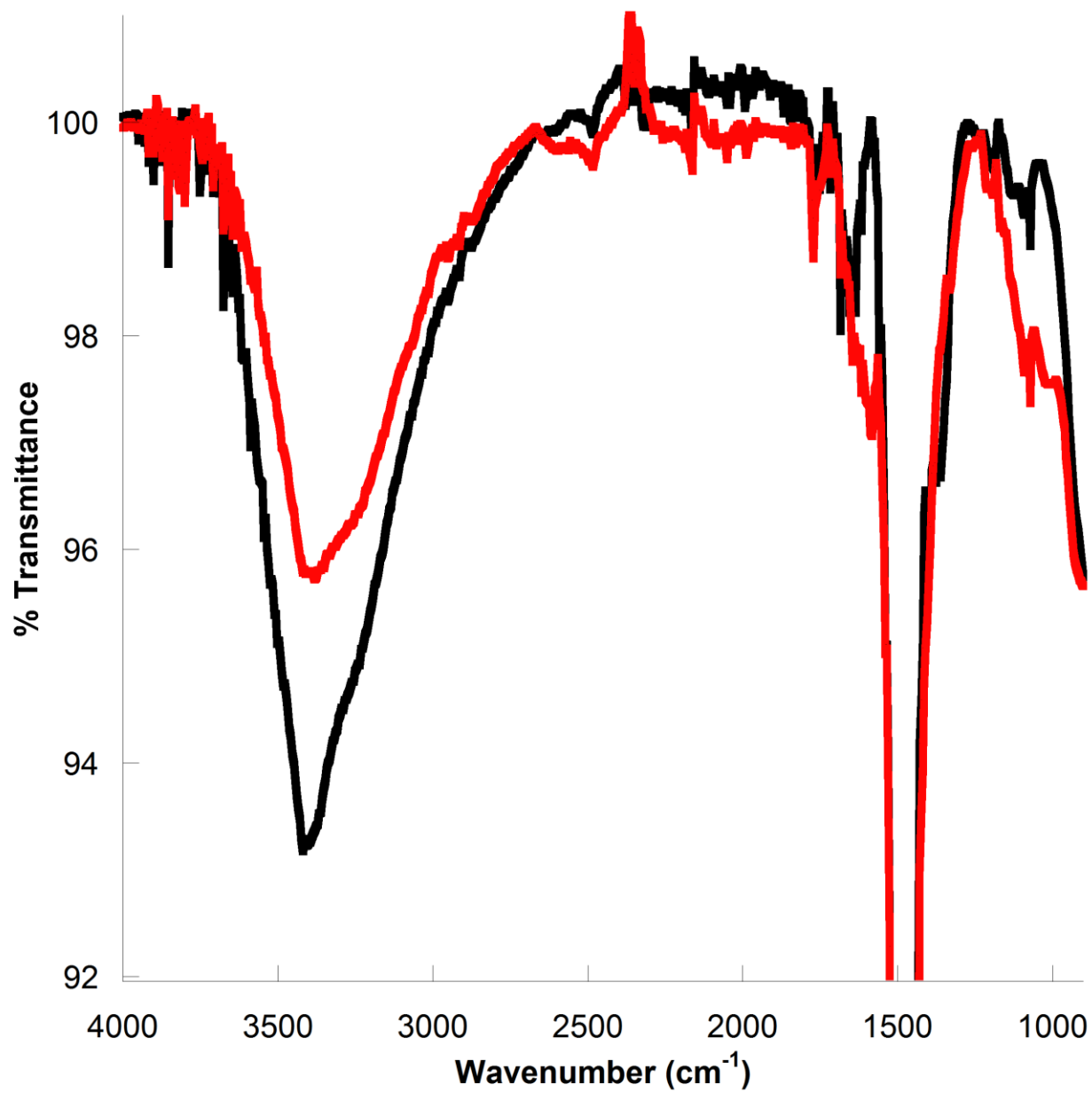


Figure S14. Powder ATR-FTIR spectra of SrTiO₃ (black) and SrTiO₃ sensitized with fluorescein (red).

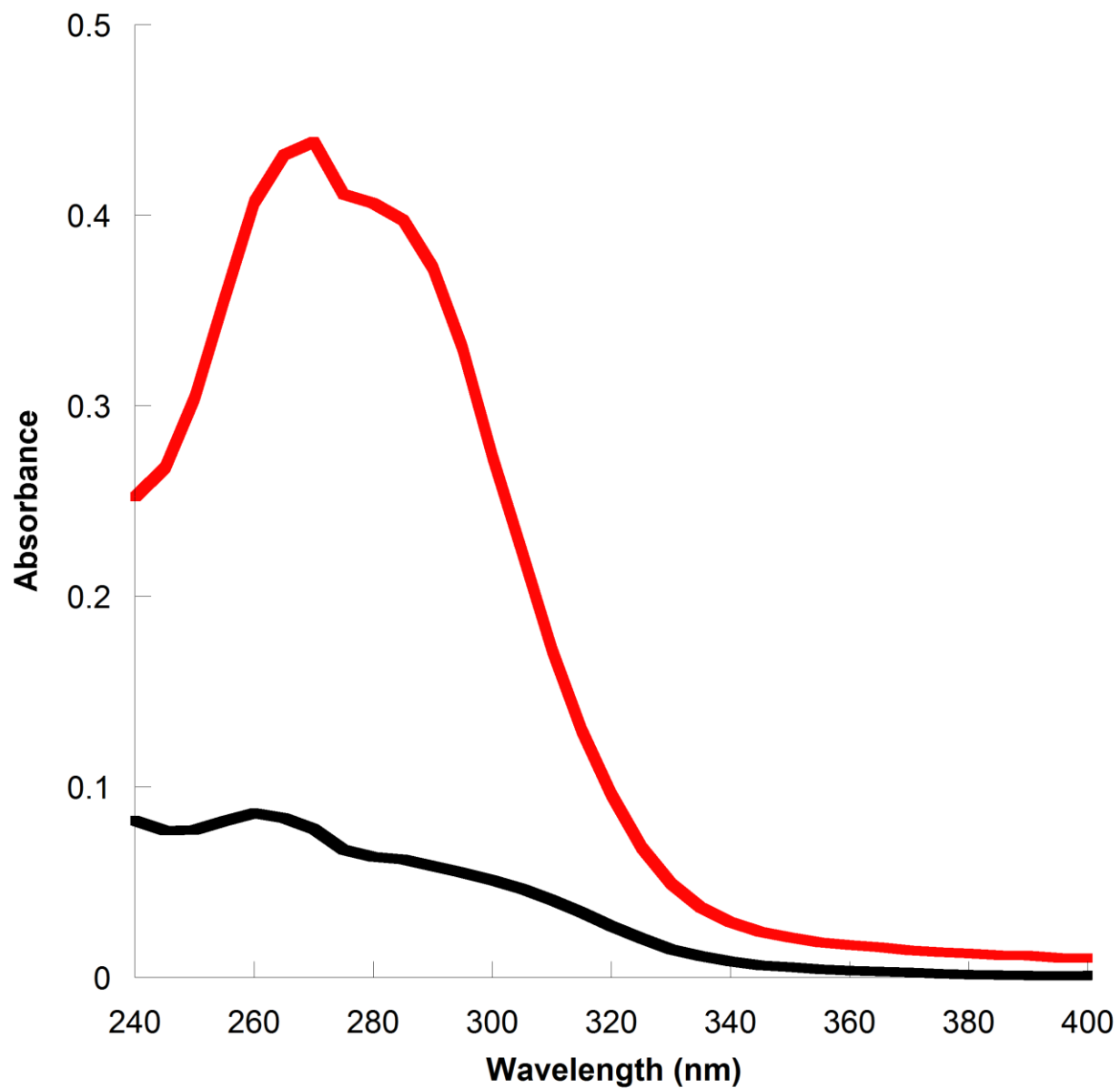


Figure S15. UV-Vis spectra of original solution of **2** (red) and supernatant collected after stirring with TiO_2 (black). Difference in absorbance at 295 nm used to determine moles of ligand immobilized on TiO_2 .

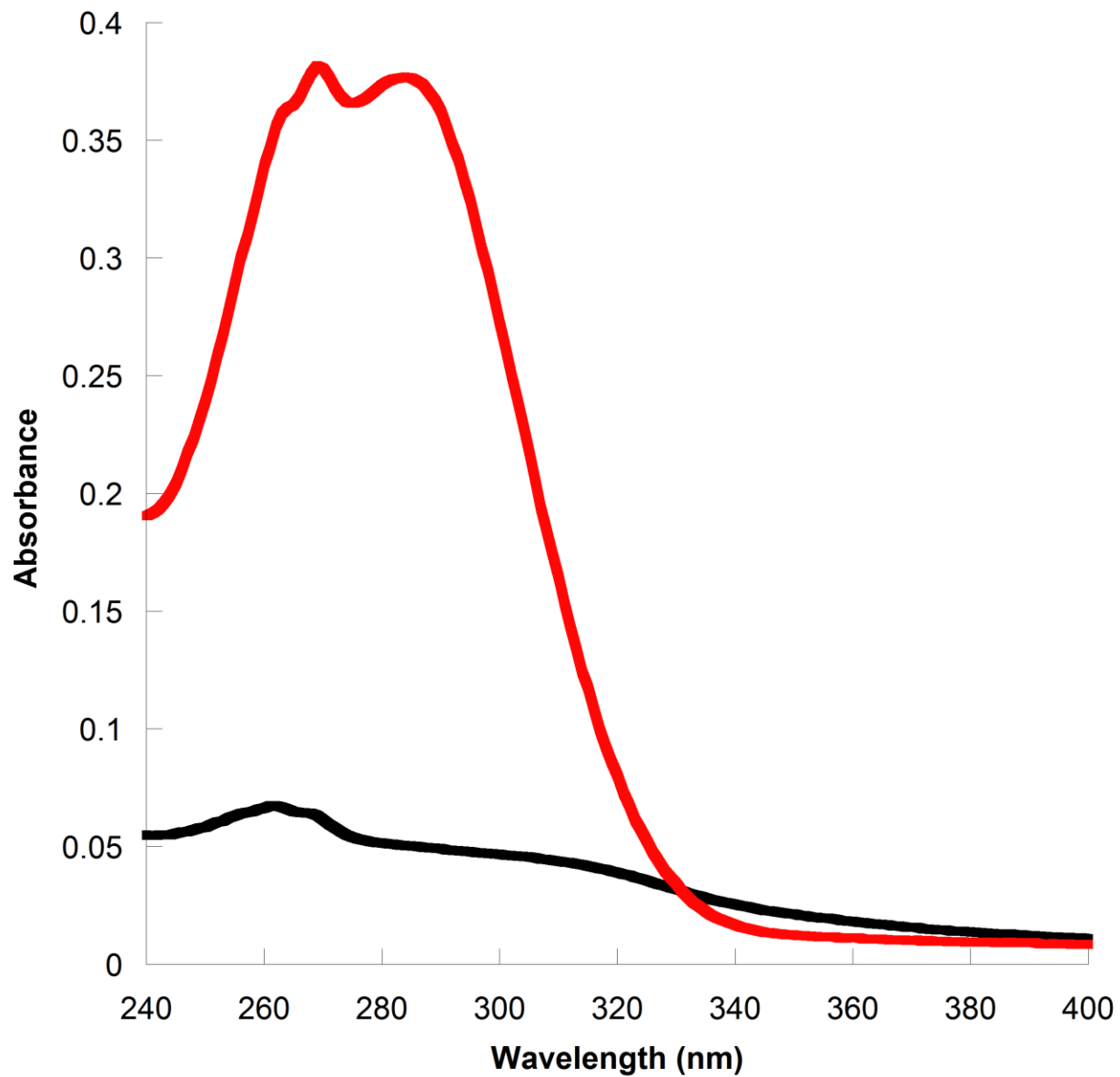


Figure S16. UV-Vis spectra of original solution of **2** (red) and supernatant collected after stirring with SrTiO₃ (black). Difference in absorbance at 295 nm used to determine moles of ligand immobilized on SrTiO₃.

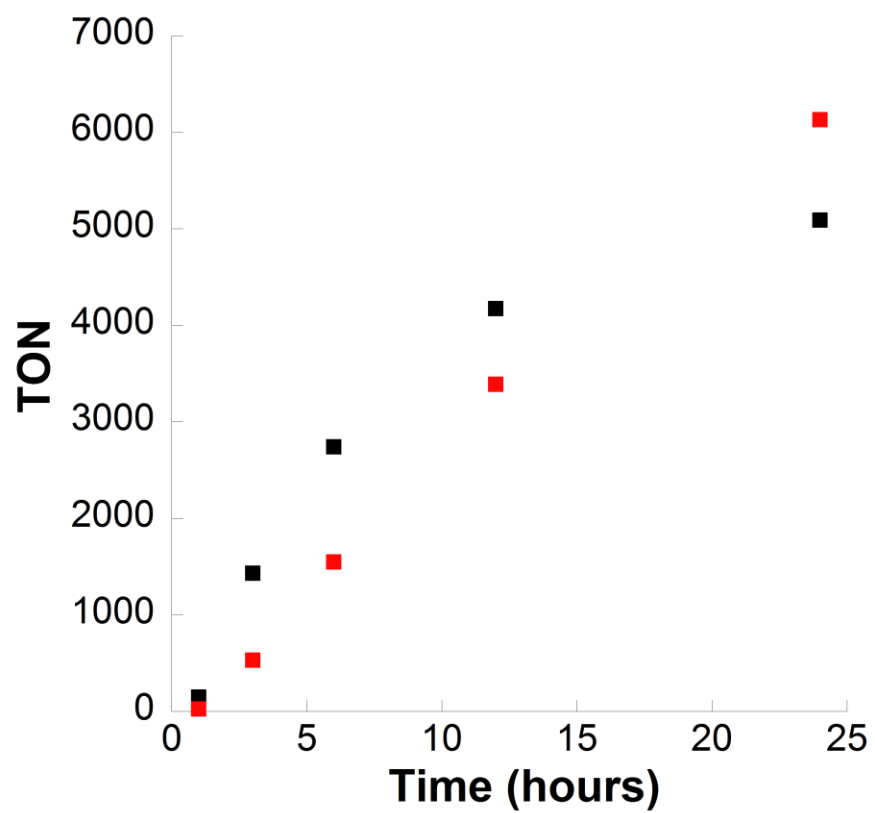


Figure S17. Hydrogen generation expressed as TON from 3-TiO₂ (black) and 3-SrTiO₃ (red) with 2 mM fluorescein and 5% (v/v) TEA in 1:1 ethanol:water corresponding to the data in Table S1.

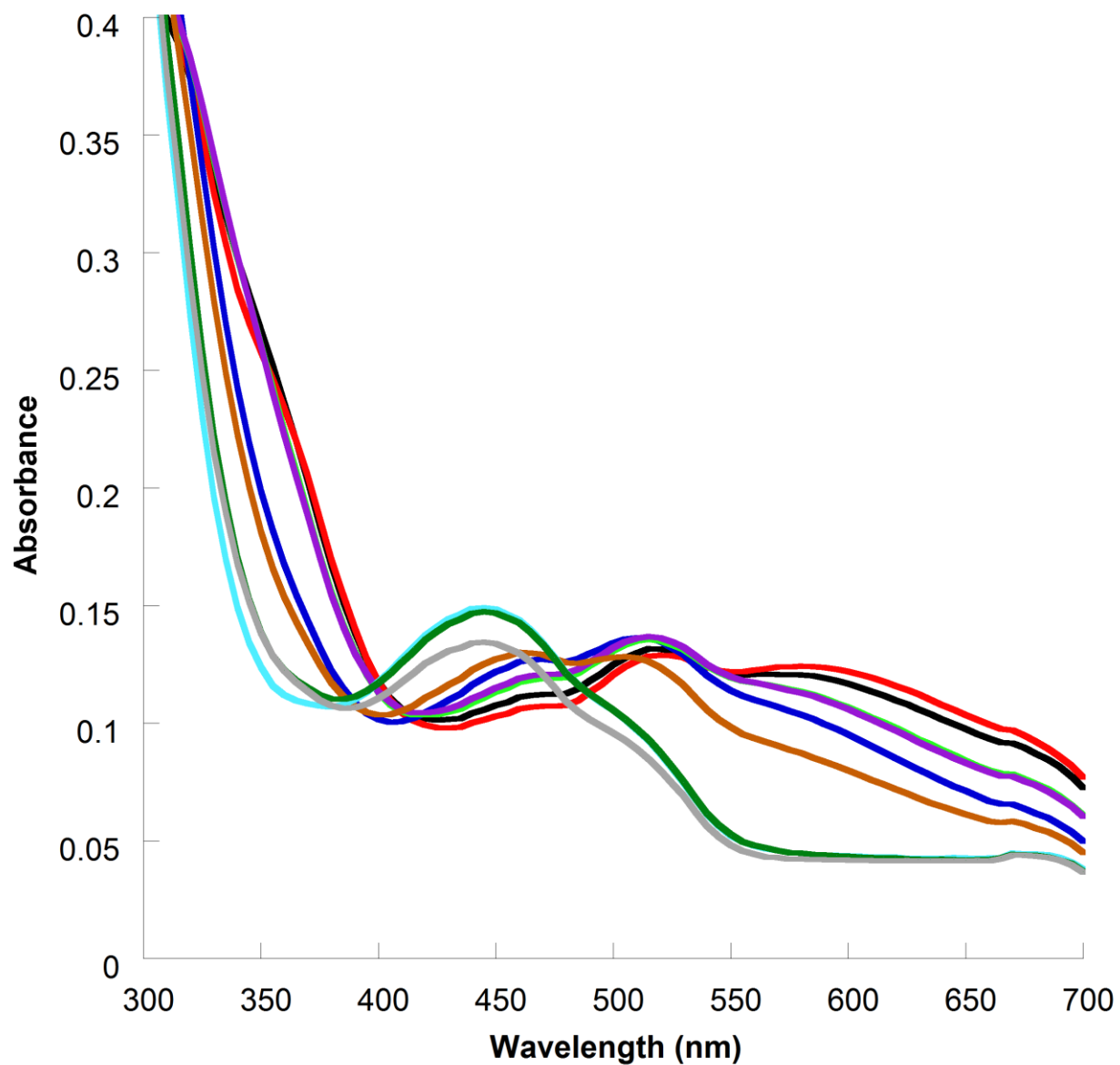


Figure S18. UV-Vis spectra of 6×10^{-5} M **1** in 1:1 ethanol:water adjusted to pH 4 (black), pH 5 (red), pH 6 (dark blue), pH 7 (light green), pH 8 (purple), pH 9 (brown), pH 10 (light blue), pH 11 (dark green), and pH 12 (gray).

Nanoparticle Description	1 mg Nanoparticles		5 mg Nanoparticles	
	H ₂ Generated (μL)	TON	H ₂ Generated (μL)	TON
3-TiO ₂	2300	6100	2700	1400
3-SrTiO ₃	1900	5000	2100	1100

Table S1. Optimization of mass of nanoparticles for hydrogen generation. Results after 24 hours of irradiation when paired with 2 mM fluorescein and 5% (v/v) TEA.

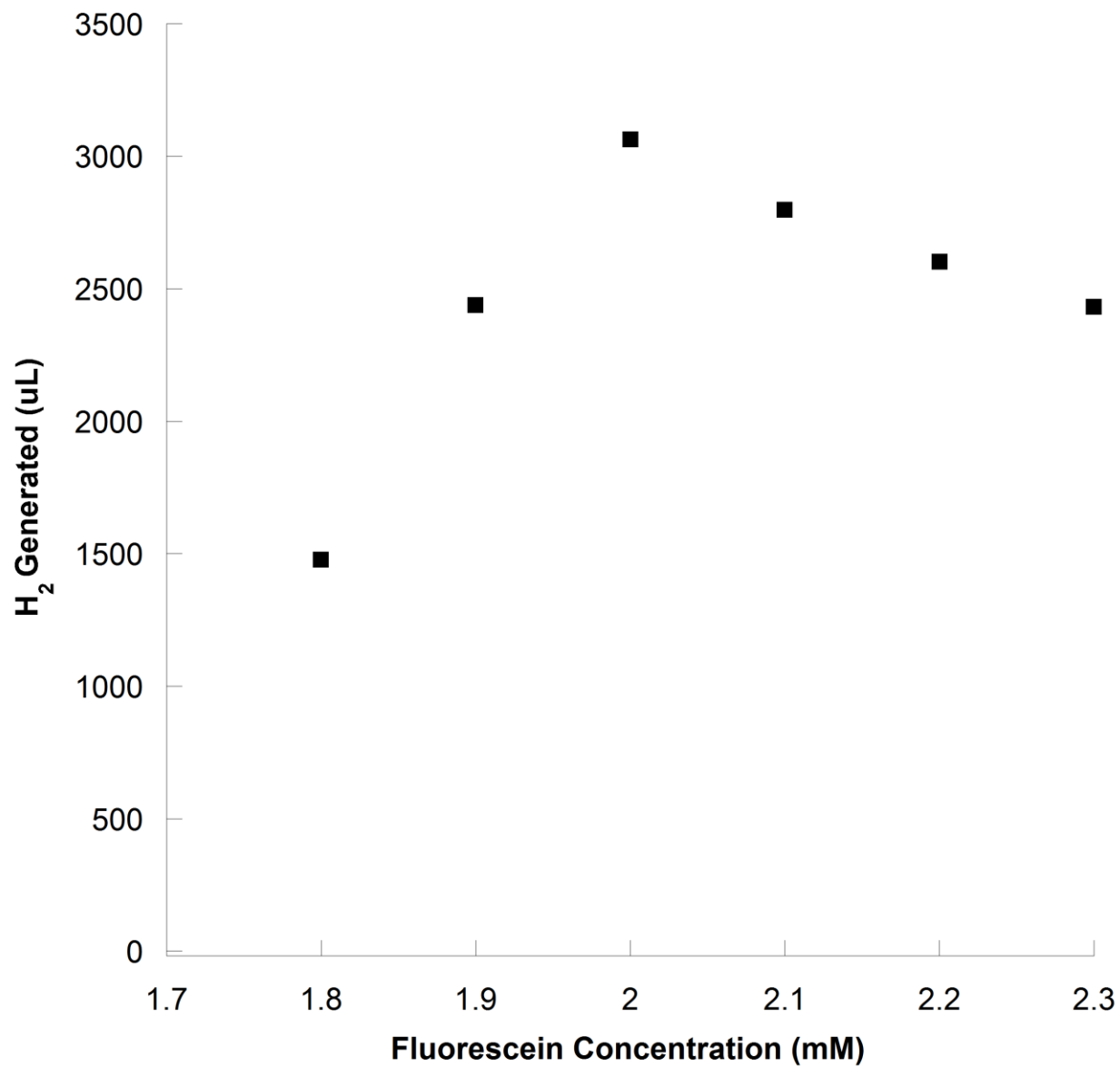


Figure S19. Hydrogen generation from 3-SrTiO₃ as a function of fluorescein concentration. Results after 24 hours of irradiation when paired with 5% (v/v) TEA.

Nanoparticle Description	H₂ Generated (μL)
3-TiO ₂	2300
TiO ₂	37
2-TiO ₂	150
Fe-TiO ₂	230
3-SrTiO ₃	1900
SrTiO ₃	81
2-SrTiO ₃	360
Fe-SrTiO ₃	90

Table S2. Hydrogen generation of additional control experiments. Results after 24 hours of irradiation when paired with 2 mM fluorescein and 5% (v/v) TEA.

Nanoparticle Description	pH of Sacrificial Donor Solution	H₂ Generated (μL)	TON
3-TiO ₂	9	0	0
3-TiO ₂	10	190	500
3-TiO ₂	11	1400	3500
3-TiO ₂	12.5	2300	6100
3-TiO ₂	13	220	600
3-TiO ₂	13.5	130	350
3-SrTiO ₃	9	1.4	4
3-SrTiO ₃	10	200	500
3-SrTiO ₃	11	550	1400
3-SrTiO ₃	12.5	1900	5000
3-SrTiO ₃	13	950	2500
3-SrTiO ₃	13.5	310	800

Table S3. Optimization of pH of sacrificial donor solution for hydrogen generation. Results after 24 hours of irradiation when paired with 2 mM fluorescein and 5% (v/v) TEA.

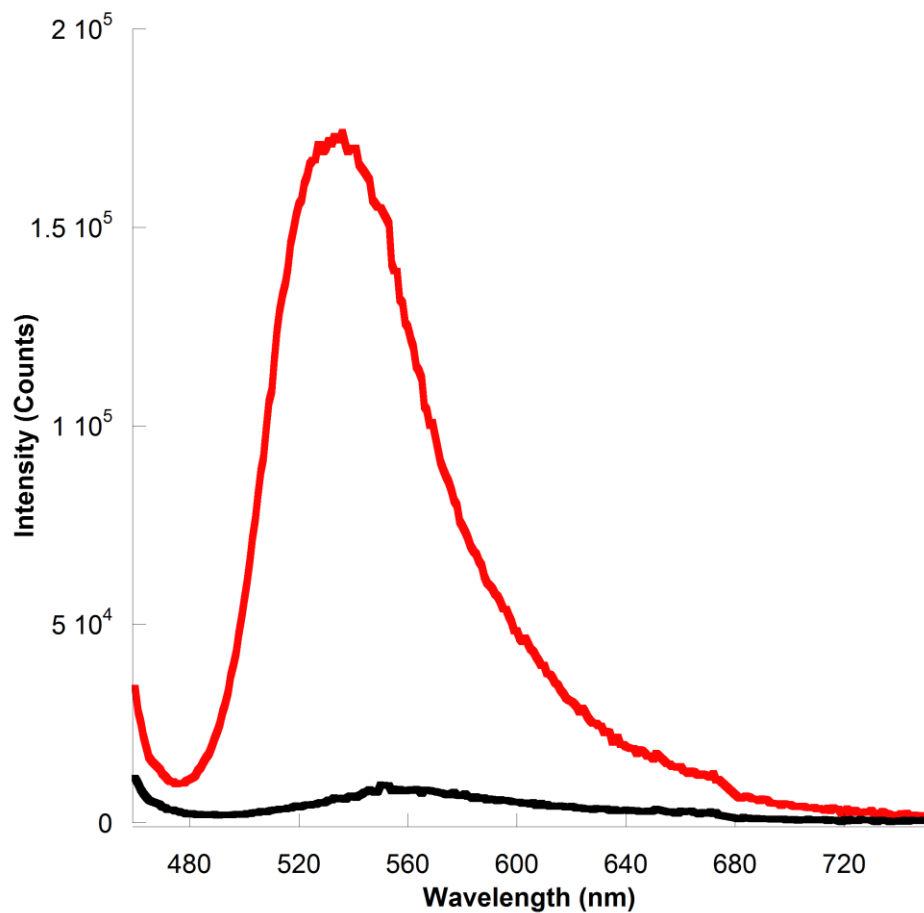


Figure S20. Emission spectra of fluorescein on TiO₂ (black) and fluorescein on SrTiO₃ (red). The emission intensity of fluorescein on TiO₂ is significantly quenched, suggesting more efficient injection into the bandgap of the semiconductor.

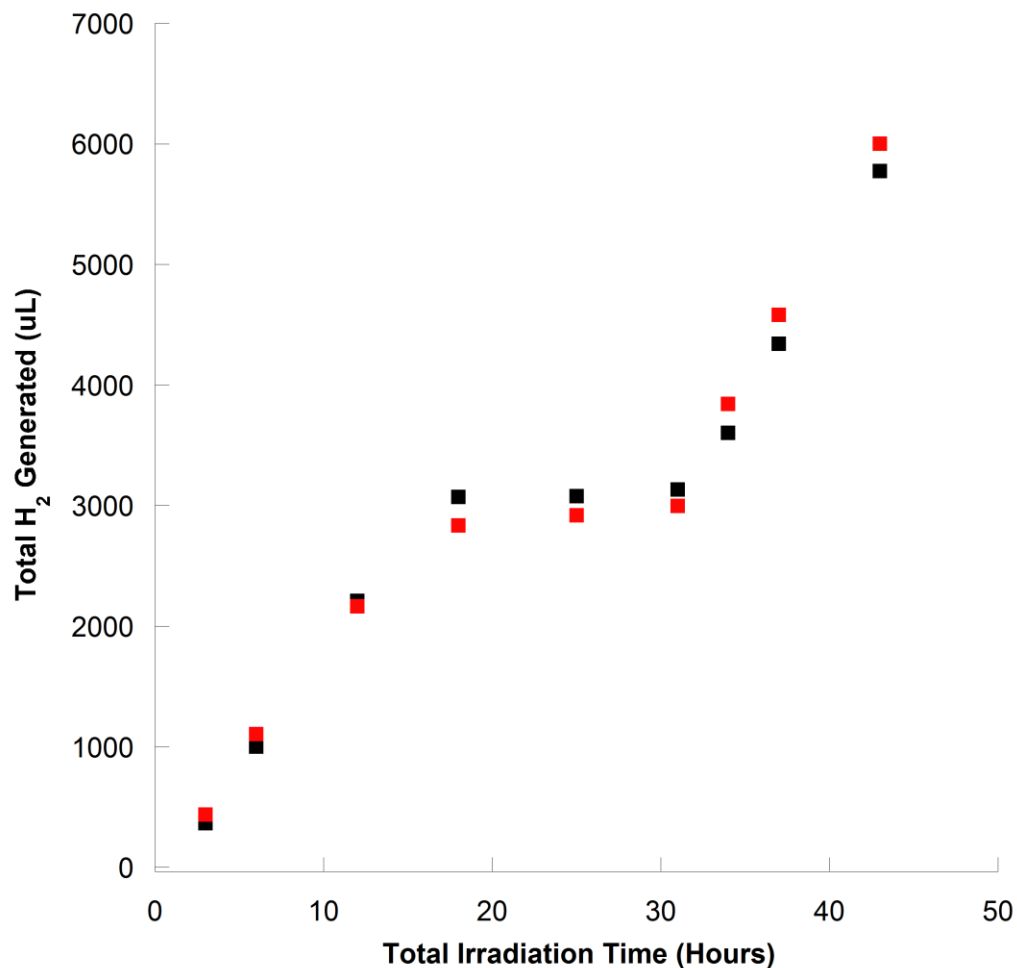


Figure S21. Hydrogen generation from 5 mg of 3-TiO₂ (black) and 3-SrTiO₃ (red) with 2 mM fluorescein and 5% (v/v) TEA in 1:1 ethanol:water. After 31 hours of irradiation, the nanoparticles were collected and the solution was discarded. The nanoparticles were then rinsed with ethanol and combined with fresh fluorescein and TEA. When irradiated further, the nanoparticles continued to generate hydrogen.

References

- (1) W. R. McNamara, R. C. Snoeberger III, G. Li, J. M. Schleicher, C. W. Cady, M. Poyatos, C. A. Schmuttenmaer, R. H. Crabtree, G. W. Brudvig, V. S. Batista, *J. Am. Chem. Soc.* **2008**, 130, 14329-14338.
- (2) G. P. Connor, K. J. Mayer, C. S. Tribble, W. R. McNamara, W. R., *Inorg. Chem.* **2014**, 53 (11), 5408-5410.
- (3) D. Talukdar, S. Panda, R. Borah, D. Manna, *J. Phys. Chem. B* **2014**, 118 (27), 7541-7553.
- (4) Y. C. Kim, S. G. Brown, T. K. Harden, J. L. Boyer, G. Dubyak, B. F. King, G. Burnstock, K. A. Jacobson, K. A., *J. Med. Chem.* **2001**, 44 (3), 340-349.
- (5) J. Warnan, J. Willkomm, J. N. Ng, R. Godin, S. Prantl, J. R. Durrant, E. Reisner, *Chemical Science*, **2017**, 8, 3070-3079.
- (6) Wise, C. F.; Liu, D.; Mayer, K. J.; Crossland, P. M.; Hartley, C. L.; McNamara, W. R. *Dalton Trans.* 2015, 44, 14265-14271.